INVESTIGATION OF CLOUD PROPERTIES AND ATMOSPHERIC PROFILES WITH MODIS

SEMI-ANNUAL REPORT FOR JULY - DECEMBER 2000
Paul Menzel, Steve Ackerman, Chris Moeller, Liam Gumley, Richard Frey, Jun Li,
Bryan Baum, Shaima Nasiri, Jeff Key, Suzanne Wetzel, Tom Rink,
Xia Lin Ma and Dan LaPorte.
CIMSS at the University of Wisconsin
Contract NAS5-31367

ABSTRACT

In the last six months, UW has worked to improve the MODIS calibration, to assure that the pre-processing algorithms are generating viable level 1b data, and to study cloud and atmospheric products generated from the science algorithms. Problems with the infrared calibration were characterized and adjustments were tested. The cloud mask was adjusted to conform with MODIS instrument performance. The UW cloud and clear sky properties were compared with those from HIRS, AMSU, and GOES; the ozone code was adjusted. The MODIS direct broadcast capability was established in August and real time images and products are starting to flow.

TASK OBJECTIVES

MODIS Atmosphere Profiles

An updated version of the MODIS Atmospheric Profiles retrieval algorithm was delivered to SDST on 26 September 2000. A new statistical retrieval algorithm developed by Jun Li at CIMSS was used; results showed major improvements in the retrieved temperature, total preciptable water (TPW), and total ozone products. Future work will focus on improving the global TPW accuracy and the total ozone accuracy in polar regions.

MODIS Infrared Calibration

UW continues to assess MODIS performance relating to sensor issues (e.g. minimizing electronic cross-talk and 5 µm leak influences on 1.38 µm band 26 radiances, fine tuning PC LWIR band optical cross-talk, investigating the effects of switching from A to B side electronics, studying band 27 RSR uncertainties due to ice buildup on the radiative cooler) and to validate L1B emissive band calibration.

EOS Direct Broadcast Hardware

The hardware for the UW SSEC X-band direct broadcast ground station was installed on 5 August 2000 by vendor SeaSpace Corp. The first pass was acquired on 18 August 2000. A successful 30-day acceptance test of the system took place during December 2000, where all 146 scheduled MODIS passes (day and night) were acquired without human intervention. Automated processing of the data to Level-1B commenced in December 2000, and in January 2001 the data will be released to the public.

EOS Direct Broadcast Software

The first major update of the International MODIS/AIRS Processing Package (IMAPP) was released on 1 November 2000 (Version 1.1). This release contained calibration updates for Terra MODIS, and a new Level-0 scanning utility that verifies compliance of Level-0 input files. This utility was invaluable in testing and debugging the SSEC X-band hardware and software.

MODIS Cloud Mask

Modifications to the MODIS cloud mask were tested and implemented in v2.4.0. These include changes to the sun-glint, desert, night-time ocean, and snow detection algorithms. Three output flags were added to indicate results of the final confidence confirmation test, the nighttime ocean variability test, and the suspended dust test. Work continues on adjusting for high elevation regions including Antarctica and making more effective use of the 1.38 μm channel.

WORK ACCOMPLISHED

Atmospheric Profiles Science Software

MODIS Atmospheric Temperature and Moisture Profile Retrieval Algorithm Version 2.3.0 (for product MOD_PR07) was delivered to SDST on 26 September 2000. This version is the first major post-launch science update for MOD_PR07. An improved regression retrieval algorithm was implemented for Terra MODIS by Jun Li at CIMSS; this is adapted from the operational GOES retrieval algorithm.

The total precipitable water retrievals at regional scale compare favorably with GOES-8 over North America (Figure 1), while at global scale MODIS exhibits a wet bias (Figure 2). This bias is still to be studied and will likely be mitigated in the coming months. The total ozone retrievals at regional scale also compare favorably with GOES (Figure 3), and at the global scale compare favorably with TOMS (Figure 4), however improvements are possible in the Antarctic, where the regression database of ozone-sonde profiles is sparse. This will be addressed with a coefficient file update.

A patched version of the MODIS Level-1B reader was delivered along with MOD_PR07 because a problem was observed in 1 km bands 24, 25, and 30 over hot land surfaces (e.g. North Africa). In these cases, the earth view radiance was greater than the permitted maximum and the scaled integer value in the HDF files was set to 32767. Unfortunately, 32767 is considered valid by the default Level-1B reader. So the MOD_PR07 version of the Level-1B reader only accepts scaled integers in the range 1-32766. MCST was notified of this problem, and it was fixed in the Level-1B production software.
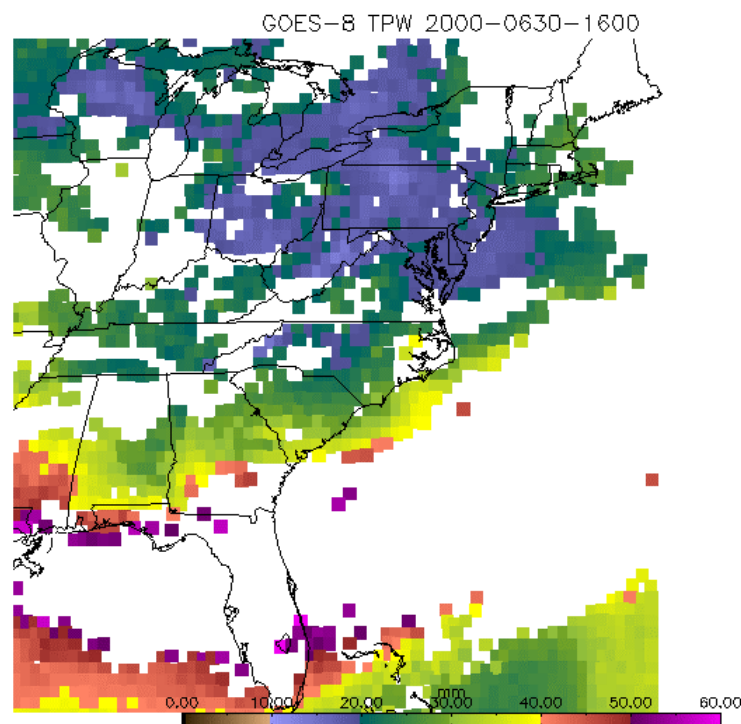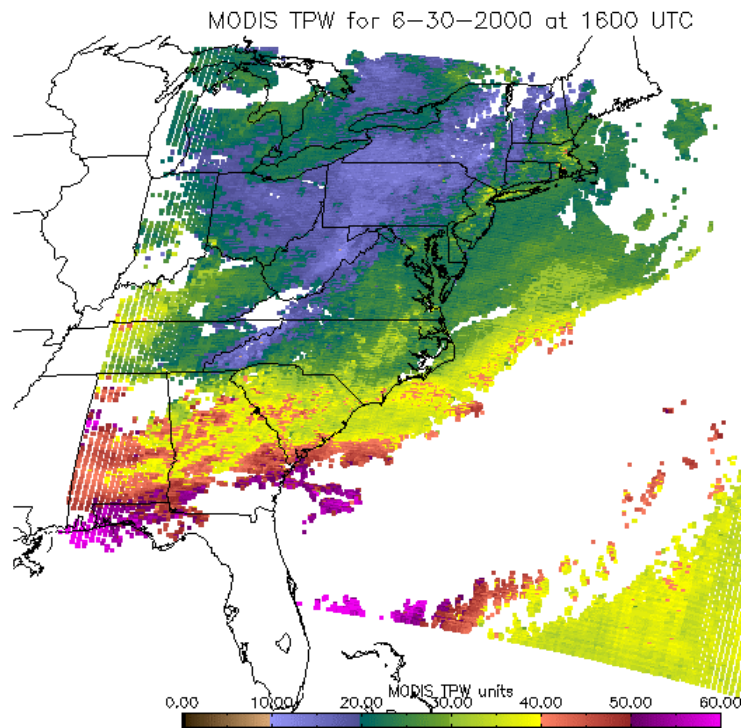
Figure 1: Regional comparison of Total Precipitable Water (in mm) derived from MODIS (top) and GOES (bottom)
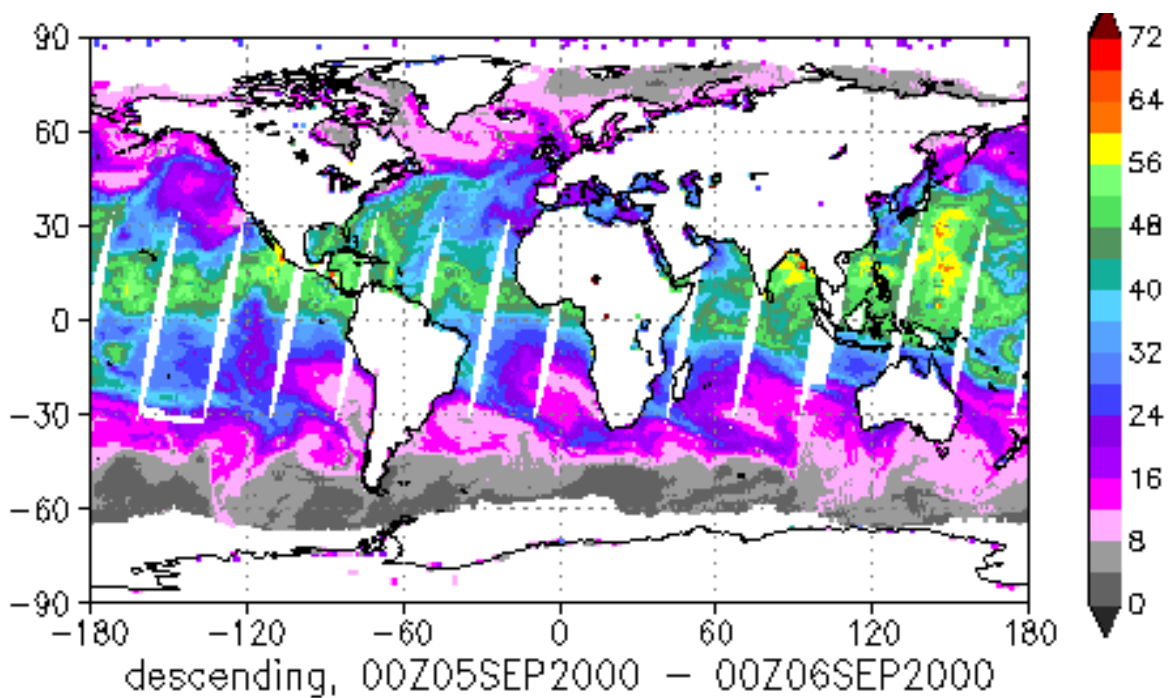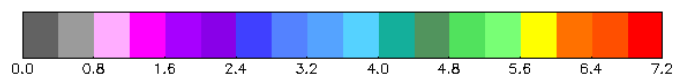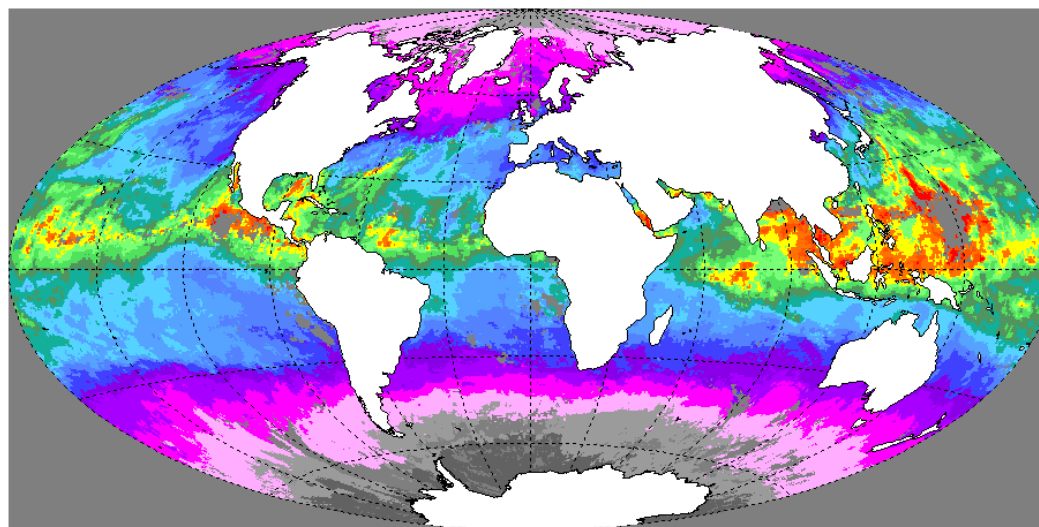
Figure 2: Global comparison of Total Precipitable Water (in cm) derived from daytime MODIS on 5-8 September 2000 (top) and NOAA-15 AMSU-A on 5 September 2000 (bottom).
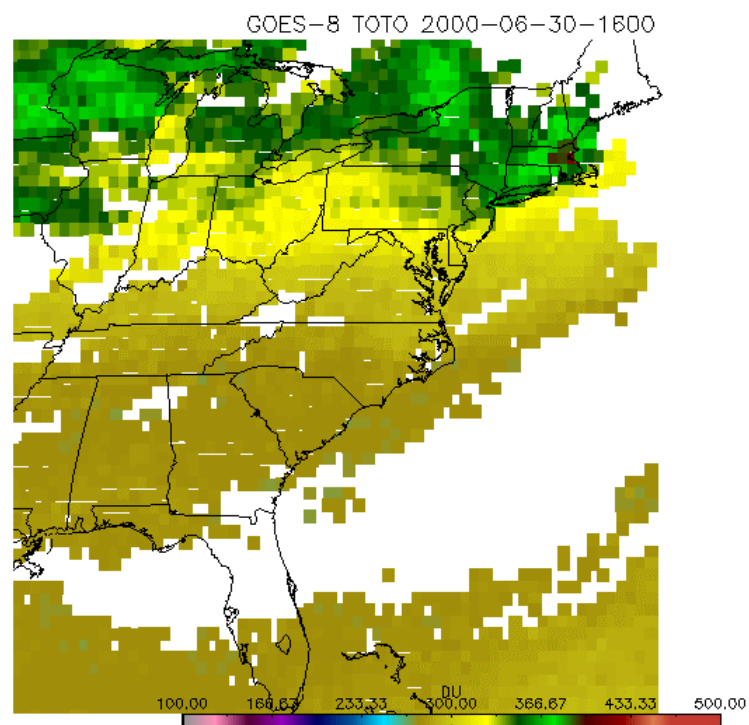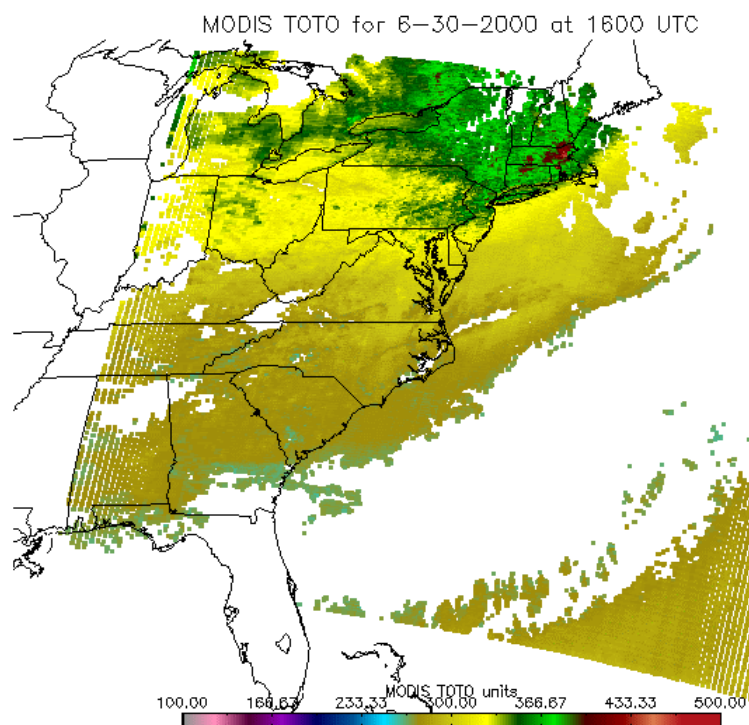
Figure 3: Regional comparison of Total Ozone (in Dobsons) derived from MODIS (top) and GOES (bottom) at 1600 UTC on 30 June 2000.
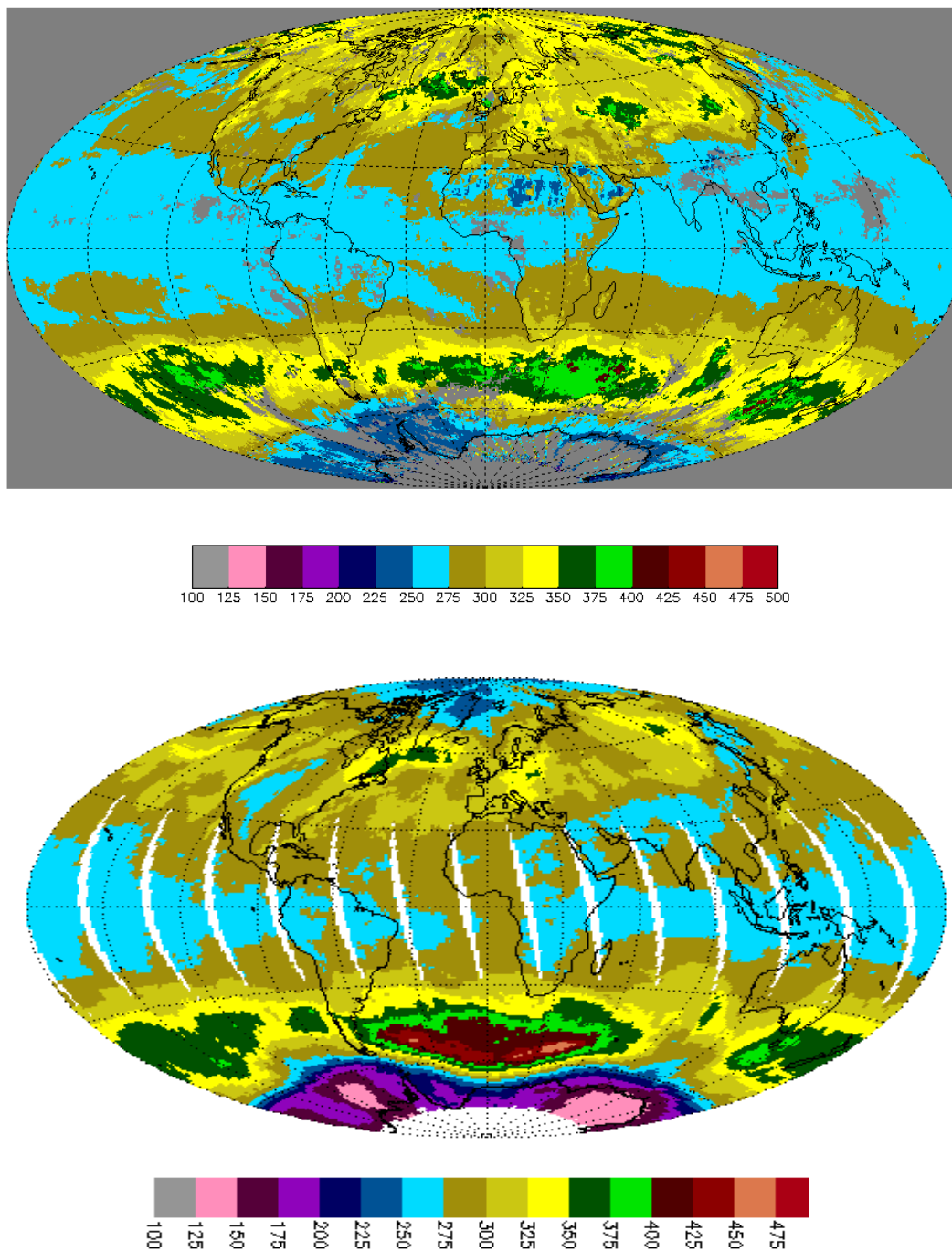
Figure 4: Global comparison of Total Ozone (in Dobsons) derived from daytime MODIS on 5-8 September 2000 (top) and Earth Probe TOMS on 5 September 2000 (bottom).

MODIS Infrared Calibration and On-Orbit Performance

The MODIS instrument performance continues to be monitored and evaluated at the University of Wisconsin. This includes testing and evaluating known MODIS performance issues as well as uncovering new performance or processing irregularities through vigilant data inspections. Whenever new irregularities are found, they are communicated to MCST. In the past two quarters these have mostly been of a minor nature associated with special modes of operating the MODIS instrument.

Understanding and improving the performance of band 26 (1.38 µm cirrus detection band) is under investigation because of its important cirrus detection capabilities in the UW MODIS cloud mask product (MOD35). Band 26 is affected by electronic cross-talk and a 5µm optical leak. Nighttime band 26 data shown in Figure 5 (processed with V2.4.4) suggests that the combination of MWIR band electronic cross-talk and 5 µm leak influences band 26 by less than 2% but contains a surface component. This surface influence, though small, introduces ambiguity between low signal thin cirrus and land surface background in daytime data (note the ghost of Cuba in Figure 5). MCST has recently installed an atmospherically based 5 µm leak correction into MODIS L1B production code (V2.5.4). It is likely that this correction can be improved by including a surface based component. Investigation suggests that including MODIS band 24 or 25 (in addition to band 28) in the correction algorithm will reduce surface influence (Figure 6).

In late October, the MODIS instrument electronics were switched from the primary (A side) to redundant (B side) configuration. A meeting to discuss the evidence supporting this change was held in late October and the action was adopted. Subsequent data analysis conducted at UW using nighttime data suggest that the switch to B side has beneficially altered the performance of the instrument. Among the findings, MODIS band 26 noise is markedly reduced by the switch to B side (Figure 7), PC band noise is reduced by as much as 50%, and striping is much reduced. An adjustment to the electronic bias (VDET) is expected to reduce the impact of electronic cross-talk in SMWIR bands, as suggested by the reduction in overall band 26 nighttime signal after Nov 1. In addition, the VDET adjustment resurrected several detectors that had been "dead" under the previous VDET bias setting. MODIS performance since these changes is encouraging, though further reduction of apparent out-of-band signal in daytime SWIR band 26 data is desirable.

MODIS PC band cross-talk correction continues to be investigated. Using earth scenes of strong contrasting thermal conditions along Baja California, an adjustment to the PC_XT cross-talk correction coefficient for band 36 (14.2 µm) has been evaluated. Since the band 36 in-band signal does not include surface influence, any representation of surface features in band 36 imagery is likely due to an 11µm optical leak into band 36. Test results indicate that the current operational PC_XT coefficient of 2.5 is under-correcting the 11 µm influence. A new PC_XT coefficient of 3.0 is recommended. Data analysis suggests that this coefficient is accurate to within about +/- 0.2; this translates to an error influence on band 36 of about 1%. This is encouraging since the pre-launch estimate of the optical leak into band 36 exceeded 10%.
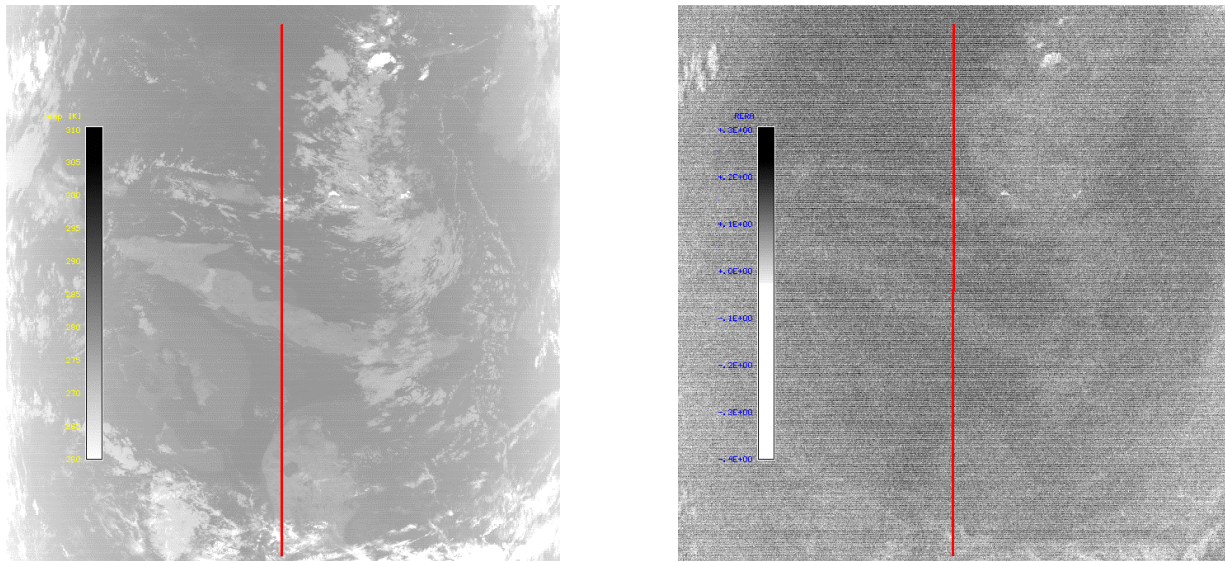
Figure 5: MODIS band 25 (4.6 µm, left) and band 26 (1.38 µm, right) nighttime imagery (07 Nov 0345 UTC) over Cuba and the Caribbean Sea. At night, the reflectance dominated band 26 signal should be near zero. However, ghosts of Cuba and Florida are visible in the band 26 imagery and are correlated to that shown in band 25. The signal level of the ghosts in band 26 is less than 0.1 W/m2 sr um, placing the contribution between 1 and 2% of the typical radiance observed in band 26. Work is underway to reduce or eliminate this out of band influence on band 26 and other SWIR bands.
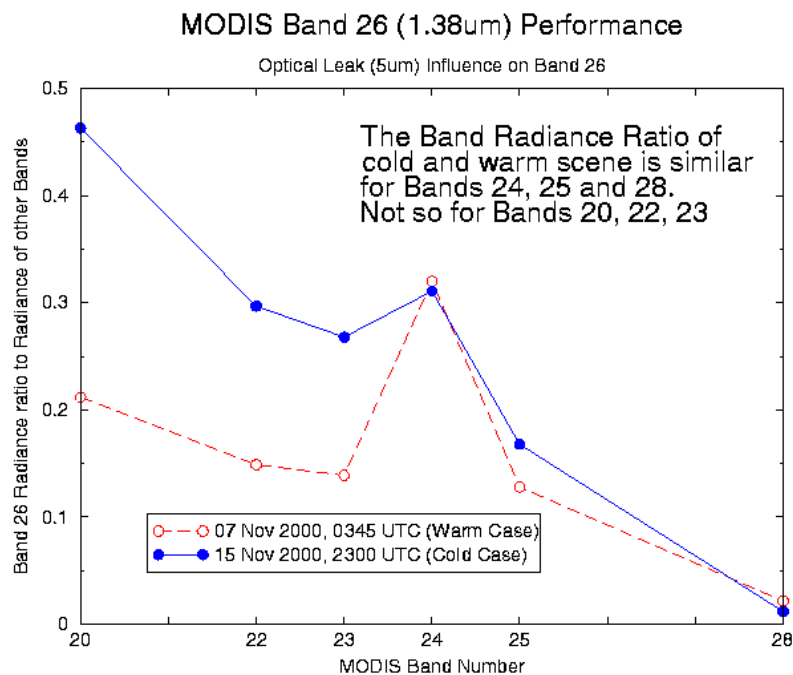
Figure 6: Using two contrasting nighttime scenes (Arctic and sub-tropical), consistency was tested between the relationship of MODIS bands 20-25 and 28 radiances to band 26 (1.38µm) radiances. Consistency in the ratio suggests a constant influence by a given band on band 26. In this test, bands 24 (4.47µm), band 25 (4.55µm), and band 28 (7.34µm) all demonstrate consistency, indicating that these bands are good candidates to correct the optical leak from the 5µm region into band 26 (and band 5, 6, and 7 as well).

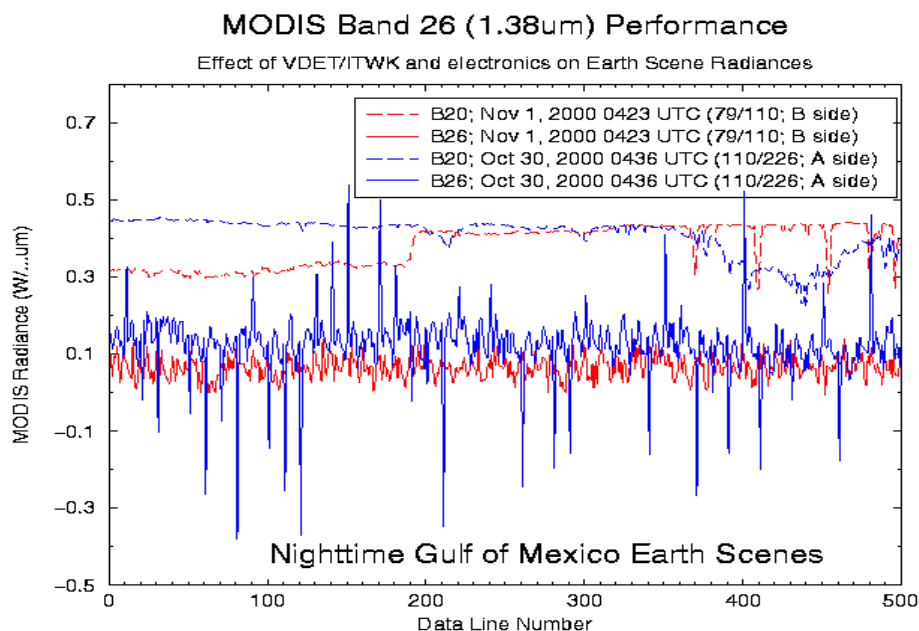**Figure 7:** Comparison of MODIS band 26 radiances before (Oct 30) and after (Nov 1) switch from A side to B side electronics and adjustment of VDET bias. The Nov 1 band 26 data (red) shows much less spike noise (striping) in this along track profile, with overall noise reduced to about 1/3 the noise of Oct 30. Overall signal on Nov 1 is also reduced (about ½ of that on Oct 30), suggesting a reduction of electronic cross-talk influence. It is important to note that nighttime data does not include possible electronic cross-talk influence from other reflectance bands in the SWIR region. SWIR bands likely continue to influence band 26 during daytime conditions.
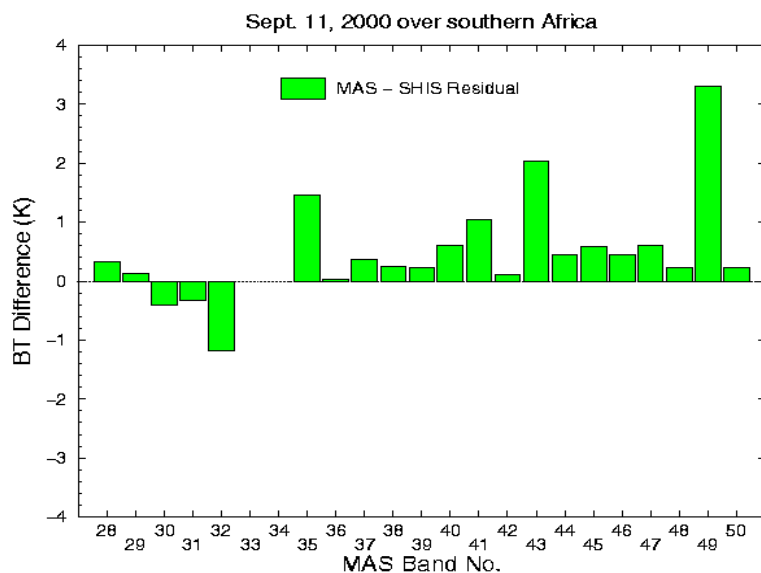
MAS Band	Central Wavelength
28H	3.48
29W	3.64
30W	3.77
31W	3.94
32W	4.10
33C	4.21
34C	4.36
35C	4.55
36W	4.70
37W	4.86
38H	5.00
39H	5.15
40H	5.29
41H	5.38
42W	8.54
43O	9.68
44W	10.46
45W	10.95
46W	11.95
47H	12.81
48C	13.19
49C	13.73
50C	14.18

Figure 8: Over 10000 MAS-SHIS calibrated brightness temperature comparisons were found in clear scenes of land and ocean on 11 September 2000 (SAFARI-2000). Spectral position is given at right (W = Window, H = H_2O; C = CO_2; O = O_3). Most MAS window bands have biases of 0.5° C or less, which is consistent with March 2000 results (not shown). Most MAS atmospheric band biases are less than 1°C, except for the Ozone band (43) and one CO_2 band (49). Those biases may be larger than expected due to spectral calibration error. Bands 33 and 34 not shown because spectral characterization is incomplete.

The temperature of the MODIS cold focal planes (SMWIR, LWIR) was observed to warm during June to early August 2000. Warming of the detectors above the 83K control point results in floating nonlinear responsivity. The warming was suspected to be have resulted from ice buildup on the radiative cooler, causing a drop in heat dissipation by the cooler. At peak impact, the MODIS cold focal plane detectors reached a temperature of about 84K, which has been estimated to cause about a 1°C error in the band 31 (11µm) calibrated brightness temperature. An additional effect of the ice buildup was that MODIS band 27 RSR and thus band 27 radiometric calibration was influenced by the intermediate stage window temperature. Transmission through this window, a function of window temperature, expands to shorter wavelengths as the window temperature rises. The estimated effect has been to increase the FWHM band-pass of band 27 by about 3% to the shorter wavelength side. Forward model calculations place this influence at about 0.15°C on the calibrated band 27 brightness temperature. To eliminate these influences, the MODIS outgas heaters were activated in early August to drive off ice buildup on the radiative cooler. That event was successful but subsequent monitoring suggests that ice buildup is again occurring. Currently the temperature of the cold focal planes remains under control at 83K, however margin in controlling at 83K has been diminishing and telemetry data suggest that the intermediate stage window temperature has been rising. This behavior is being closely monitored and documented by MCST. For data sets between June and early August, a correction algorithm is intended to address the drifting detector temperature issue. A correction algorithm to mitigate the ongoing influence of the intermediate stage window temperature on band 27 RSR is under development at MCST.

A NASA ER-2 aircraft outfitted with MAS and SHIS under-flew Terra on 16 missions during the SAFARI-2000 field campaign in South Africa. The flight of 11 September 2000 (flight 00-160) includes clear scenes over ocean with Terra directly overhead. The data from MAS and SHIS is being analyzed for MODIS emissive band radiometric calibration comparisons. In the process, SHIS calibration is transferred to MAS and MAS data is convolved over the MODIS spatial weighting function. Dependence on small spectral variation between MAS and MODIS emissive bands is removed using a radiosonde profile in a forward model. A correction for the altitude difference between MAS (20 km) and MODIS (705 km) is also applied. The 11 September 2000 comparisons are of interest because they represent the first opportunity to evaluate MODIS radiometric performance after the early August outgas activity. Results of this comparison will be available in the first quarter of calendar 2001 and will be presented at the 2001 SPIE annual meeting.

MAS IR Calibration Studies

The SAFARI-2000 field experiment has provided a data set to evaluate MAS thermal emissive band radiometric performance. MAS calibration is routinely maintained by NASA ARC through annual blackbody emissivity measurements, spectral calibration before and after field deployments, and optics maintenance. Monitoring MAS calibration accuracy over time contributes to the overall knowledge of sensor and component behavior as well as supporting important vicarious calibration activities for MODIS and other sensors. The UW has been active in assessing the thermal emissive band calibration of MAS for several years through comparisons with HIS and SHIS. Calibration comparisons between MAS and SHIS from 11 September 2000 data show that MAS thermal emissive window and atmospheric

bands continue to be well calibrated (Figure 8). LWIR window bands are within 0.5°C agreement with SHIS. Most atmospheric bands are within 1°C agreement; however the ozone sensitive band 43 and CO_2 sensitive band 49 show unexpectedly large biases, possibly due to spectral calibration errors in these atmospheric bands. These results are largely consistent with those found from comparisons during the WISC-T2000 field experiment (March 2000), indicating that MAS thermal emissive band radiometric performance is stable and that the implemented proactive maintenance program is effective.

MODIS Direct Broadcast Hardware

A significant milestone was reached when the SeaSpace TeraScan SX-EOS ground station was installed on the rooftop of the SSEC building on 5 August 2000. General contractors J.P. Cullen & Sons and airlift specialists Carson Helicopters provided installation and lift services. The antenna was assembled on the ground, and the radome enclosure was then built around the antenna. The radome and enclosed antenna were then lifted by helicopter to the top of the tower which had been installed previously (Figure 9). During August and September 2000, the finishing touches were made to the tower. Electrical service, lighting, and walkways were completed. The radome is rated to handle 150 mph wind loads. The antenna is completely shielded from winds, rain, and snow by the radome, which allows work to be done on the antenna in relatively comfortable and safe conditions. A GPS receiver on the antenna platform relays accurate time codes to the control computer located on the 6th floor of the SSEC building, where the antenna controller, receiver, control computer, disk array, and UPS are located.

The first pass from Terra MODIS was acquired on 18 August 2000 (Figure 10), and since then, between 4 and 6 passes per day have been acquired. On 29 December, SSEC completed the 30 day acceptance test of the SeaSpace system. The system was required to automatically acquire all Terra passes (day and night) during this period without any human intervention. A total of 146 passes were acquired successfully during the test, which happened during the snowiest December on record for Madison (it was also the 4th coldest December on record). SSEC is now routinely processing the data to Level-1B via the International MODIS and AIRS Processing Package (IMAPP), and will soon release the name of the FTP server where the latest 7 days of Level-1B data will always be available. In addition, a McIDAS ADDE server is pointing to the data, so McIDAS users can access it. Finally, we are planning to installs a DODS server on the same system so that others can access subsets of the data through C, FORTRAN, IDL, or Matlab.

Lifting frame test

Detail of radome and tower

4.4 meter antenna

Helicopter departs after successful lift to roof

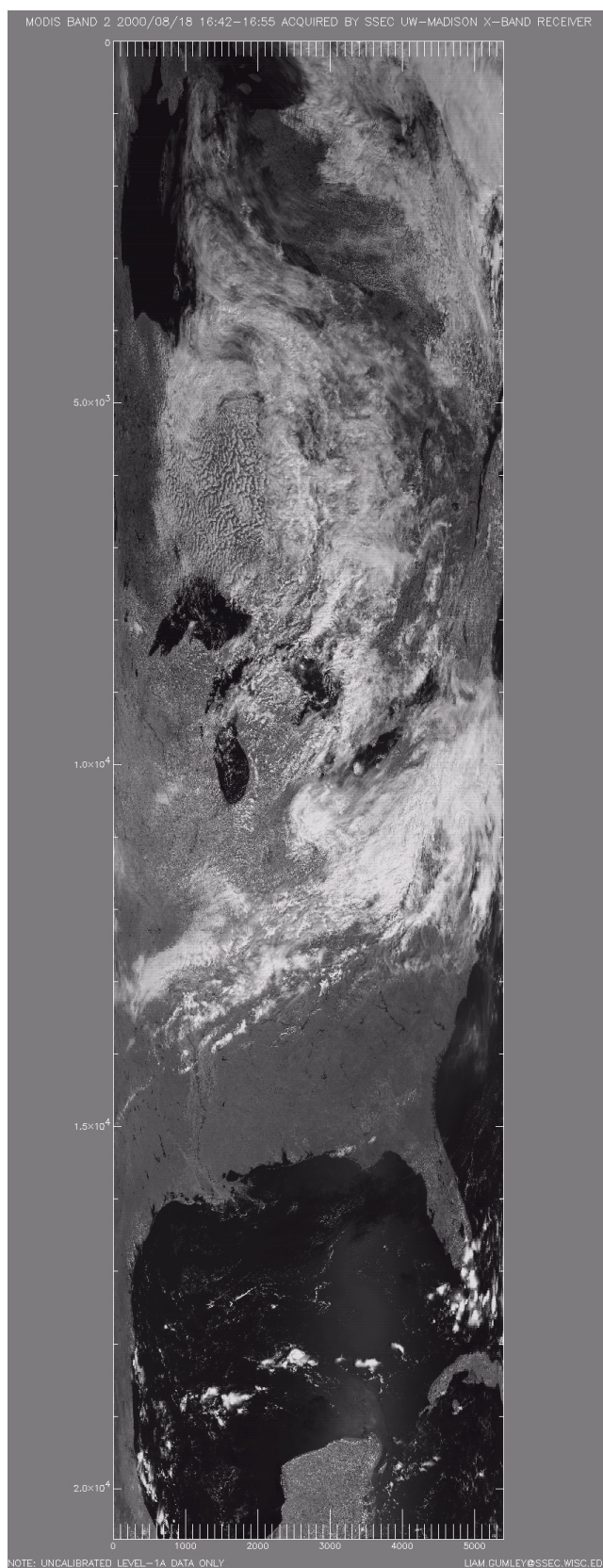**Figure 9:** MODIS Direct Broadcast Antenna Installation

Figure 10: First MODIS Direct Broadcast Pass acquired at SSEC on 18 September 2000.

MODIS Direct Broadcast Software

The International MODIS and AIRS Processing Package (IMAPP) Version 1.1 was released on 1 November 2000. This was the first major update for MODIS on the Terra spacecraft. Improvements included:

- Calibration algorithm and lookup tables are updated to Version 2.4.3. This includes many post-launch improvements and bug fixes from the MODIS Calibration Team at GSFC.

- Added support for definitive ephemeris and attitude data.

- Solarisx86 is now supported on Intel Pentium platforms.

Calibration accuracy of IMAPP Version 1.1 was evaluated as follows. MODIS Level-1B 1000 m resolution data for 2000/10/13 (day 287) from 1555 to 1600 were acquired from the GSFC DAAC, and compared to the corresponding direct broadcast data acquired at SSEC. The GSFC data were processed with the operational GSFC calibration software version 2.4.3. The SSEC data were processed with IMAPP 1.1. Every pixel in every band was compared (a total of 1354 x 2030 = 2,748,620 pixels). In all bands (1-36 at 1000 m resolution), greater than 99.998 percent of pixels had radiance differences of less than 0.1%.

For geolocation, the operational MODIS processing system at GSFC uses definitive post-processed spacecraft ephemeris and attitude information. By default, IMAPP uses the ephemeris and attitude information contained in the X-band downlink for geolocation, which may contains gaps and other anomalies. Thus the geolocation information produced by IMAPP (when the downlink ephemeris/attitude data are used) is not as robust. In addition, IMAPP does not currently support terrain correction (although this will be added in an upcoming IMAPP release). IMAPP Version 1.1 can use the definitive spacecraft ephemeris and attitude data if they are available at runtime, which significantly increases geolocation accuracy. We are establishing an archive of these data that will be accessible by anonymous FTP, and we will notify the community when the data are available. Keep in mind that the definitive ephemeris/attitude data are often not available until at least 24 hours after direct broadcast reception. Finally, we are investigating predictive ephemeris approaches that will allow improved geolocation at the time of data reception.

MODIS Cloud Mask

An updated version of the MODIS cloud mask algorithm was delivered to SDST on 29 September 2000. The major changes were:

- New sun-glint "final confidence confirmation test" based on a 3.75-11 um difference rather than 3.75 um brightness temperature alone. Result is reported in bit #26. In cases of severe sun-glint, confidence of clear sky is determined to be uncertain if no IR test indicates cloud.

- Additional checks for cloudy pixels misidentified as snow.

- An 11 um variability (standard deviation over 3x3 pixel region) test in night, ocean situations. Result is reported in bit #27.

- New daytime desert "final confidence confirmation test". If no IR cloud test indicates cloud, and the 11 um brightness temperature is higher than a given threshold, then pixel is determined to be clear. Result is reported in bit #26.

- New "suspended dust test". Test is performed in daytime, land surface situations. Result is reported in bit #28.

- No shadow determinations are attempted in coastal regions.

- Negative radiance values from band 26 are "valid".

- If radiance data from any channel normally used in sun-glint regions is not valid, no determination of clear-sky confidence is made.

- Various cloud test thresholds were adjusted.

- Bit #s 26-28 were added to the cloud mask output:
  # 26 final confidence confirmation test
  # 27 nighttime ocean variability test
  # 28 suspended dust flag

Many of these changes were motivated by suggestions from various users of the cloud mask data set. For example, members of the MODIS Land Science Team reported problems in desert areas and also suggested not making shadow determinations near coastlines. Investigations of atmospheric aerosols led to the adjustment of visible band thresholds in daytime land situations in order to detect more boundary layer clouds and work on cloud properties revealed problems in sun-glint regions.

Efforts to improve the cloud mask have continued since the September 2000 update. High altitude surfaces (with no snow) can have remarkably different spectral characteristics than other clear-sky regions. Work is in progress to insert an elevation check in the cloud mask and then to use adjusted visible and near-IR cloud test thresholds in cases where the altitude is higher than a specified value.

Another effort is to make better use of the 1.38 μm band. It has been found that over oceans one can significantly lower the band 26 cloud test threshold from its original value and in turn improve cloud detection. The amount of this decrease and the impact on the final cloud mask product is being evaluated.

Code has been developed which composites cloud mask output data over an arbitrary number of granules. Composites may be made of any parameter within the MOD35 output file including individual cloud test results contained in single bits. Figure 11 shows example output where the frequency of cloud (confidence of clear sky < 66%) is shown for daytime data on 5 November 2000. Individual pixel values were accumulated on a 25 km equal-area grid and then reduced to a 0.5 degree equal-angle grid for display.
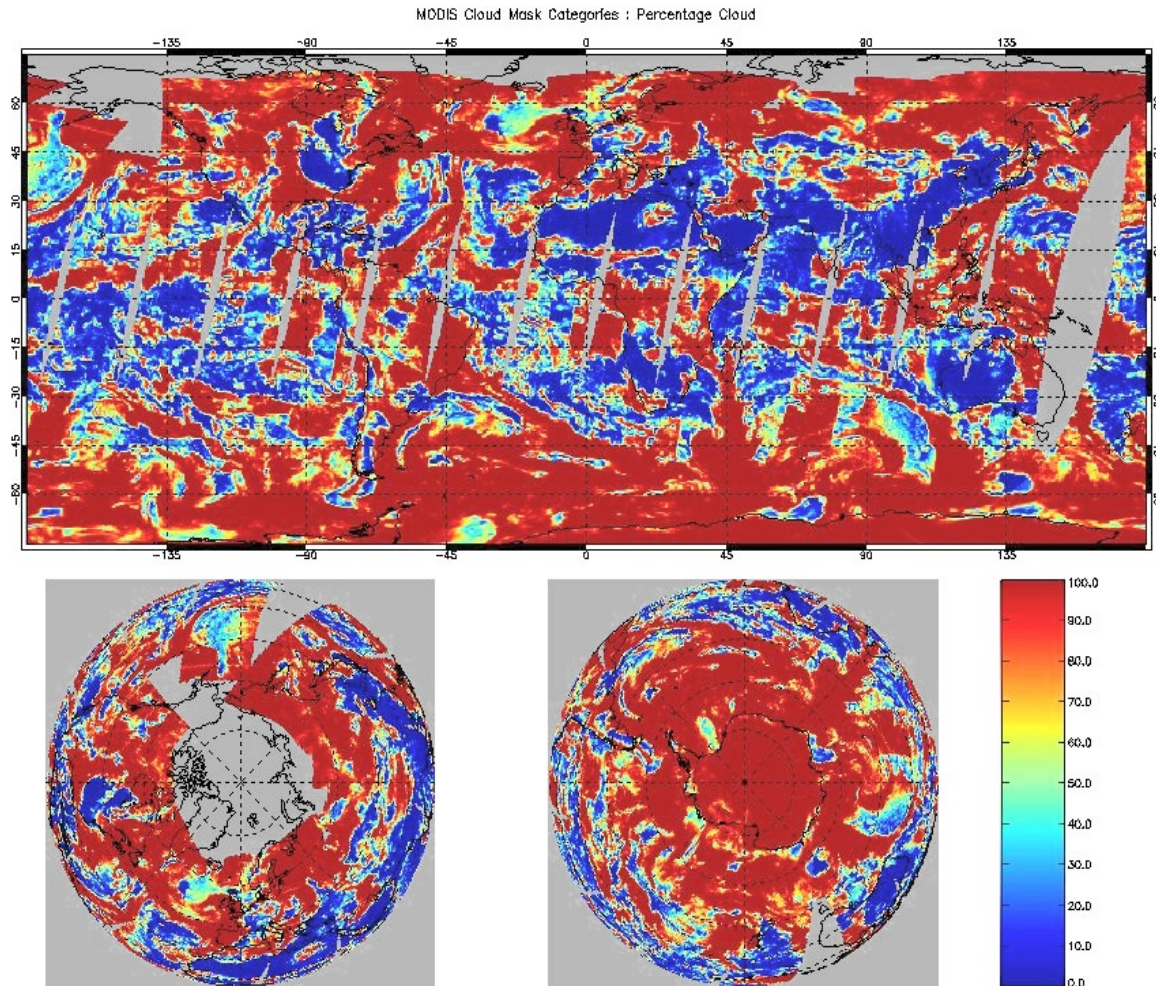
Figure 11: Global daytime cloud frequency for 5 November 2000. Results from the MODIS cloud mask where the confidence of clear-sky was < 66%.

Cloud detection in the polar regions is being carefully evaluated. Currently implemented cloud test thresholds perform well in daytime polar data, and we do not anticipate any significant changes in the near future. However, nighttime cloud detection, especially over high elevation and extremely cold areas such as Antarctica and Greenland, has a much higher degree of uncertainty. Recent improvements in polar cloud detection with the AVHRR are being tested with MODIS data. The 11-12 μm brightness temperature difference test that has been widely used to detect thin cirrus at temperatures above 260 K has been extended to temperatures as low as 190 K. This brightness temperature difference is strongly dependent upon the scene temperature through its correlation with atmospheric water vapor, and it is also a function of sensor view angle. Figure 12 illustrates the temperature dependence for clear sky, nadir views; the view angle dependence is not shown. Threshold functions that have been successfully applied to the detection of thin cirrus and "warm" clouds in AVHRR data are also shown. This test is being evaluated for use in detecting clouds at night over snow and ice. The quality of the 3.9 μm band at very low temperatures is also being investigated.
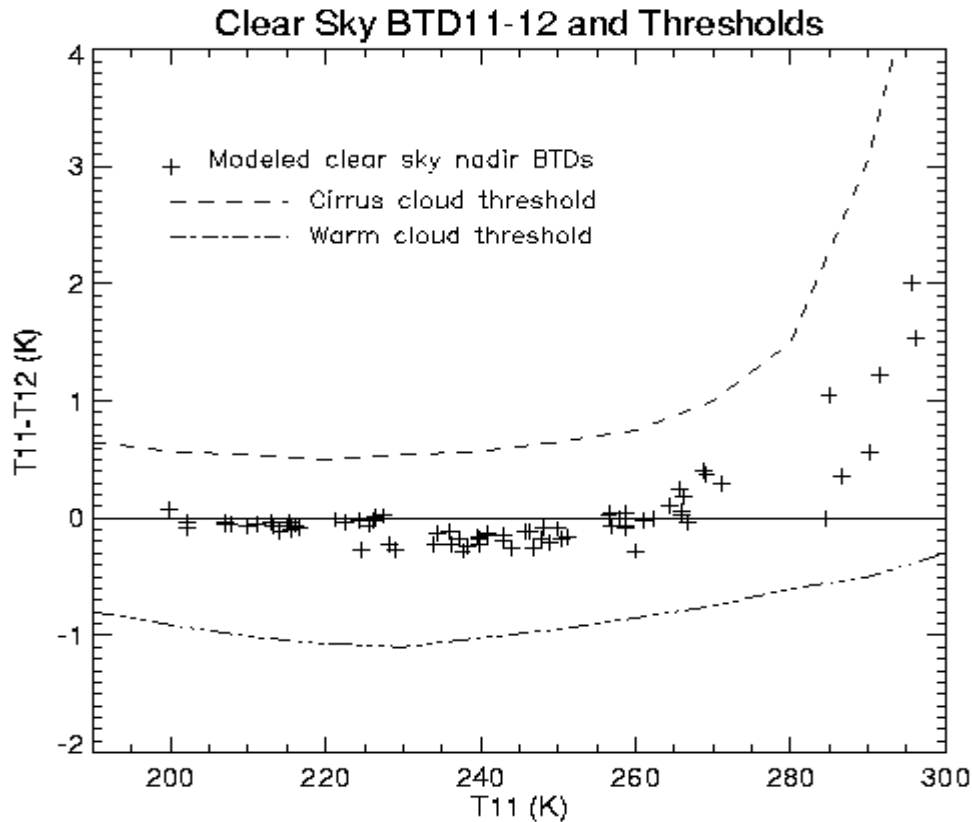
Figure 12: Modeled clear sky brightness temperature differences at 11 and 12 μm over a broad range of temperatures. Also shown are thresholds functions that have been used in the polar regions for detecting cirrus clouds (dashed line) and clouds that are warmer than the surface (dot-dash line).

ER-2 Activities

Plans are moving forward for a spring 2001 deployment based in San Antonio, TX projected for 14 March – 5 April. The ER-2 payload is planned to include MAS, SHIS, CPL, AirMISR, and MOPITT-A along with a camera system. A possible coordination with the UND Citation for cloud validation activities is included in the plans and enhanced surface based measurements with an up and downlooking AERI instrument are under consideration for the ARM Central Facility. In addition to MODIS validation work (clouds, atmospheric water vapor, L1B radiances, coastal turbidity), the objectives list has expanded to include MOPITT and MISR validation and cirrus cloud microphysical studies. All science flights during this field activity will be coordinated with Terra overpasses.

DATA ANALYSIS

Cloud Top Properties

Several modifications were made to the MODIS cloud top properties algorithm during the past six months. While the original MODIS IR cloud phase algorithm was tested extensively with MODIS Airborne Simulator data, the algorithm was found to have some problems with the lower-resolution MODIS data. The maximum likelihood estimator method sometimes

returned inconsistent results in scenes where broken low clouds were present. The algorithm was redesigned in order to mitigate this problem. Thresholds were also altered due to changes in calibration. Work continues on modifications that will allow the use of solar and/or near-infrared bands in daytime situations.

Code was created in order to correlate MODIS IR cloud phase retrievals with other MODIS cloud top properties, including cloud top temperature. In operational processing (MOD06), the IR cloud phase and cloud top temperature (from the CO_2-slicing algorithm) are computed separately so that analyzing the correlation between them could yield insights into either one or both computations. Figure 13 shows percentages of total retrievals on 5 September 2000 where water clouds (as determined by the IR phase algorithm) are found in conjunction with cloud top temperatures > 273K. Results were tabulated for water backgrounds during both day and night from 60 south to 60 north latitude and are displayed on a 0.5 degree equal-angle grid. Percentages are quite high over much of the world oceans as expected, but some very cloudy regions display much lower values. High frequencies of water clouds with cloud top temperatures below freezing in the ITCZ and mid-latitude storm tracks probably indicate the presence of many mid-level super-cooled water clouds.

In-house MOD06 code was modified in order to investigate the effects of resolution on output cloud top properties products. This version of the cloud top properties algorithm may generate products at spatial resolutions from 1 to 20 km (single-pixel retrievals up to a 20x20 pixel box). The analysis of output data sets is continuing.
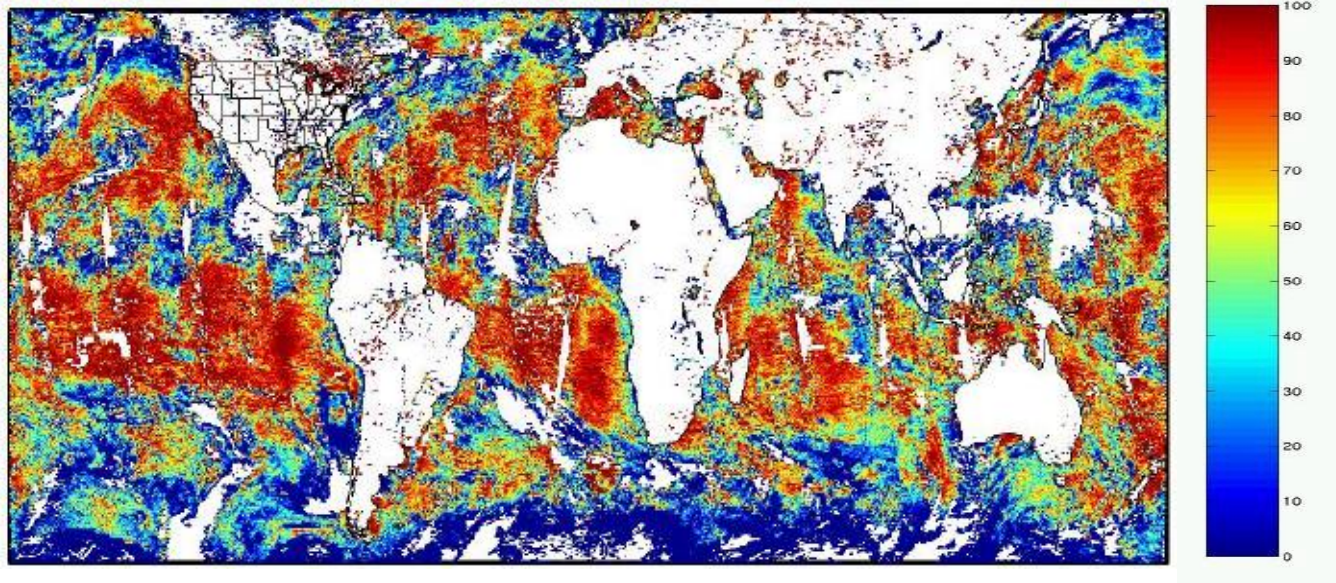

Figure 13. Map showing frequency of occurrence of warm (cloud top temperature > 273K) water clouds. Colors represent the percent of total retrievals where water phase clouds as derived by the MODIS IR phase algorithm correspond with warm clouds as determined by the MODIS CO_2-slicing algorithm.

MODIS – GOES Intercomparison

Comparisons between the 6.7 and 11-μm GOES and MODIS brightness temperatures have been started. To account for the difference in spatial resolution between the two instruments, clear-sky radiance data are first binned and averaged to a 25-km equal-area grid. Radiative

transfer calculations are performed to correct for differences between the GOES and MODIS spectral response functions. Corrections for viewing zenith angle differences between the two satellites are also made to enable comparison over any clear-sky ocean scene near the equator. Temperature and humidity profiles, skin temperature, and surface pressure from GDAS 1° global data serve as input to the forward model. The software to perform these various tasks has been automated using Matlab and can be extended to compare any two satellites' radiance and product data.

GOES and MODIS corrected and uncorrected brightness temperatures for 5 November 2000 (JD 310) at 1745 UTC and 1750 UTC, respectively, are shown in Figures 14 and 15. Each point represents the brightness temperature for a single 25-km equal area grid cell from a 5° latitude x 10° longitude box centered at approximately 2.5°N and -110°W. Figure 14 shows the 11-μm IR band results before (b) and after (a) correction for spectral response function and viewing zenith angle differences. Figure 15 shows the 6.7-μm H2O band results. Considerable agreement between the corrected brightness temperatures is evident in both bands. However, the 6.7 μm MODIS band shows a consistent cool bias of less than 1° K compared to GOES that is still under investigation.
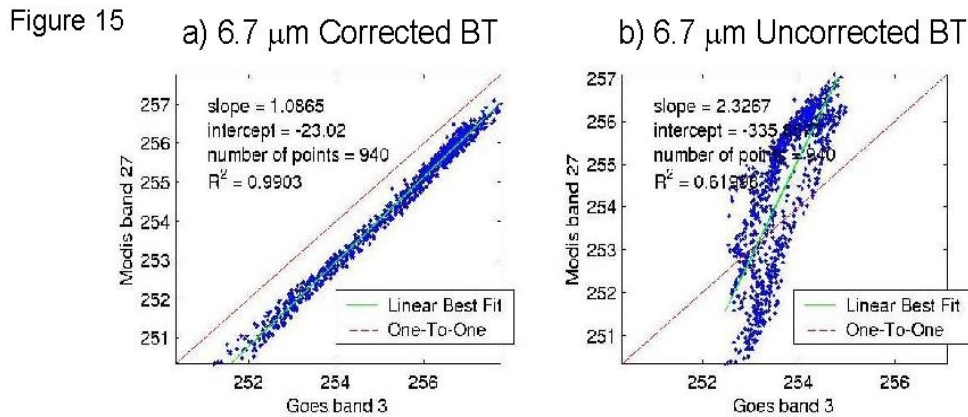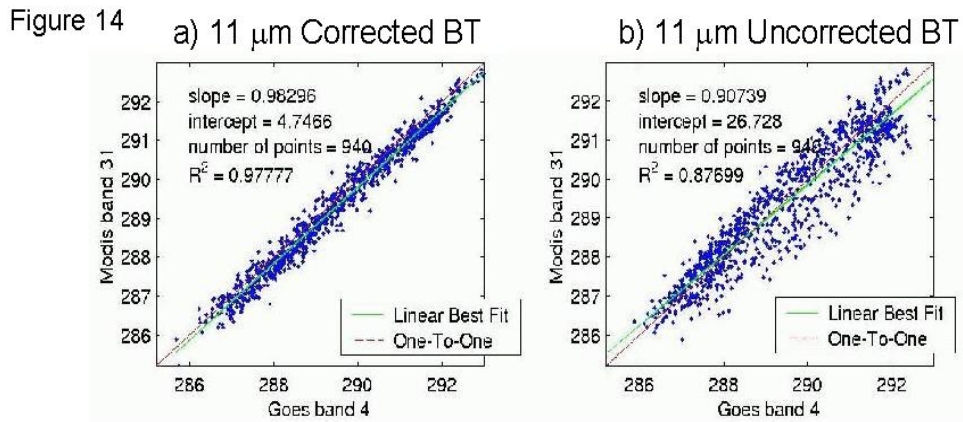

Figure 14: Comparison between MODIS and GOES 11-μm brightness temperatures for (a) data that has been corrected for spectral response function and viewing zenith differences and (b) uncorrected data. Each point represents the average brightness temperature in degrees K in a clear-sky 25km equal-area grid cell.
Figure 15: Same for MODIS and GOES 6.7-μm brightness temperatures.

MODIS Two-Step Physical Retrieval Algorithm

The two-step physical retrieval algorithm source code originally developed to retrieve atmospheric temperature-humidity profiles, surface skin temperature and surface emissivities from MAS data was updated for processing MODIS data.

• The updated source code was tested using a global data set with wide range of atmospheric and surface conditions. The global data set used is called "NOAA-88b" profiles distributed from the NPOESS Integrated Program Office (IPO). A subset of "NOAA-88b" was selected as a training data set (1765 profiles).

• The daytime training dataset was generated using the following procedure: a) surface skin temperature was from surface air temperature plus a random noise with mean = 0 and STD = 6 K; b) local zenith angle varies from 0.0 (at nadir) to 20.0 degree in steps of 5.0 degree, from 20.0 to 65.0 degree in steps of 3.0 degree; c) solar zenith angle varies from 25.0 to 85.0 degree in steps of 5.0 degree; d) solar anisotropic factor varies from 0.75 to 1.25 in steps of 0.05; and e) surface pressure is varied from 700-1050 hPa. Atmospheric and surface properties are intended to cover a wide range of likely real situations. The daytime training data set has 1,036,035 profiles.

• The night-time training dataset was constructed from the daytime dataset in the following way: a) the night-time temperature profile was generated from the daytime temperature profile by linear interpolation after cooling -6 K at 1000 hPa and no change at 500 hPa; and b) the water vapor mixing ratio profile was dried by 15% from 500-1000 hPa.

• The independent test dataset was selected from the "NOAA-88b" profiles, after removing the profiles from the training data set. 441 profiles were carefully chosen from the three zones (Middle-latitude, High-latitude and Tropical) and four seasons (Summer, Winter, Spring and Fall). A few inversion profiles in the boundary layers were also included. The surface skin temperature, local zenith angle, solar zenith angle, solar anisotropic factor and surface pressure variations in the test dataset were randomly generated.

• The surface emissivity data, consisting of band-averaged emissivities of 80 terrestrial materials, were randomly incorporated into the training and test data sets. The surface emissivity varies from 0.56 to 0.99.

A physical model to retrieve atmospheric total ozone was developed and it was incorporated into the MODIS two-step physical retrieval model as a part of the MODIS processing package. Sensitivity and error analysis were conducted using MODIS two-step physical retrieval algorithm as follows:

• Errors due to solar anisotropic factor uncertainty: currently there is no physically solar anisotropic factor (SAF) calculation model available. Thus SAF from regression retrieval was used as a true value in the physical retrieval, so it is necessary to estimate retrieval errors due to SAF uncertainty. Statistical results illustrate that there is no significant error increase in the physical retrieval when SAF uncertainty varies in a range of 10% RMS error (see columns 4 and 5 in Table 1).

• Errors due to calibration and other uncertainty: A random number with STD = 0.2 K and Mean = 0.0 K was added into the day/night MODIS simulated brightness temperature datasets to take account of sensor calibration errors, forward model calculation errors and other errors, such as pixel registration offset between multitemporal observations. It was found that the RMSE of the retrieved parameters are not significant worse compared to the retrieved results without noise (See columns 4 and 6 in Table 1)

MODIS observations in the daytime at 17:00-17:05 UTC on 17 September 2000 and in the nighttime at 04:05-04:10 UTC on the next day (Figure 16). The two data sets overlap in the central and eastern US. Data quality checks excluded "bad" sounding points in the retrieval processing. MODIS data were averaged to 10x10 fields of view (FOV). Regression and physical retrievals were applied to the collocated day/night data sets. GOES retrievals instead of RAOB data were used for validation to accommodate the 17 and 4 UTC observation times (although GOES sounding data at 03:00 UTC on Sept. 18 was used because of no data available at 04:00 UTC). Figure 17 shows the retrieved surface skin temperature from MODIS and GOES respectively in the overlap region; a good agreement is achieved, especially for the daytime data set. Figure 18 shows the results for retrieved total precipitable water vapor (TWV); MODIS TWV is capable of retrieving medium-scale atmospheric and surface variability with similar retrieval accuracies as GOES but with much higher spatial resolution. Figure 19 shows the retrieved surface emissivities within the short-wave (band 22) and long-wave (band 32). It is difficult to compare retrieved emissivity with measured surface emissivity over land if the composition of the surface is unknown. Thus for simplicity, validation is limited to Lake Michigan where the retrieved surface emissivities are approximately 0.97 and 0.98 and are close to the lab measured results.

Table 1. Retrieval rms of Independent Dataset Simulated for Daytime/Nighttime 441 Profiles, with Guess SAF and no Noise Added versus True SAF and Noise Added

	Dependent Mean profiles.	Regression Rtvl.	Physical Rtvl. (Guess SAF, no Noise Added)	Physical Rtvl. (True SAF, no Noise Added)	Physical Rtvl. (Guess SAF, Noise Added)
Layer (hPa)[a]	T (K)	T (K)	T (K)	T (K)	T (K)
Daytime					
1 (0.1-10)	8.94	5.39	5.34	5.34	5.33
2 (10-50)	6.84	2.39	2.33	2.34	2.37
3 (50-100)	8.74	3.31	3.27	3.27	3.32
4 (100-300)	4.18	1.42	1.43	1.43	1.44
5 (300-500)	10.23	1.89	1.61	1.62	1.64
6 (500-700)	11.38	1.49	1.10	1.10	1.10
7 (700-850)	12.26	1.91	1.51	1.51	1.52
8 (850-1050)[b]	13.50	3.00	2.66	2.68	2.72
Ts (K)	15.21	1.10	0.30	0.27	0.37
TPW (cm)	1.29	0.43	0.24	0.30	0.31
Nighttime					
1 (0.1-10)	8.94	5.39	5.35	5.34	5.36
2 (10-50)	6.84	2.39	2.33	2.33	2.35
3 (50-100)	8.74	3.31	3.24	3.24	3.28
4 (100-300)	4.18	1.42	1.42	1.42	1.43
5 (300-500)	10.22	1.88	1.59	1.59	1.61
6 (500-700)	11.34	1.49	1.12	1.12	1.13
7 (700-850)	12.18	1.79	1.46	1.45	1.47
8 (850-1050)[b]	13.39	2.74	2.48	2.48	2.55
Ts (K)	15.15	0.46	0.24	0.19	0.26
TWP (cm)	1.18	0.36	0.26	0.26	0.27

[a]SAF, solar anisotropic factor; Ts, surface skin temperature; TPW, total precipitable water vapor.

[b]Only 334 profiles.

Table 2. Retrieval rms of Independent Dataset Simulated for Daytime/Nighttime 441 Profiles, with Guess SAF and no Noise Added versus True SAF and Noise Added

	Dependent Mean profiles.	Regression Rtvl.	Physical Rtvl. (Guess SAF, no Noise Added)	Physical Rtvl. (True SAF, no Noise Added)	Physical Rtvl. (Guess SAF,Noise Added)
O3 (Db)[a]	51.15	27.98	19.81	19.88	20.54
ε_{20}	0.031	0.017	0.007	0.004	0.008
ε_{22}	0.033	0.018	0.007	0.004	0.009
ε_{23}	0.034	0.020	0.009	0.007	0.010
ε_{29}	0.033	0.012	0.009	0.009	0.010
ε_{31}	0.018	0.010	0.008	0.008	0.009
ε_{32}	0.014	0.009	0.010	0.010	0.012

[a]**Db, Dobson unit; $\varepsilon_{20,...,}\varepsilon_{32}$, bands 20,…,32 surface emissivities.**
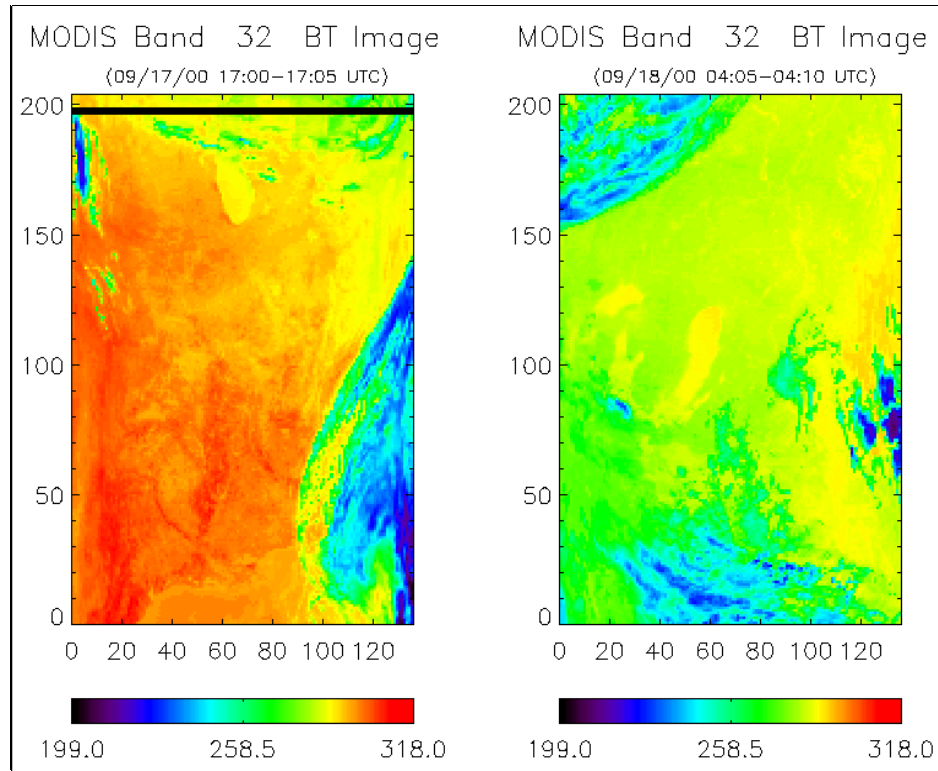

Figure 16: MODIS IR window observations in the daytime at 17:00-17:05 UTC on 17 September 2000 and in the nighttime at 04:05-04:10 UTC on the next day
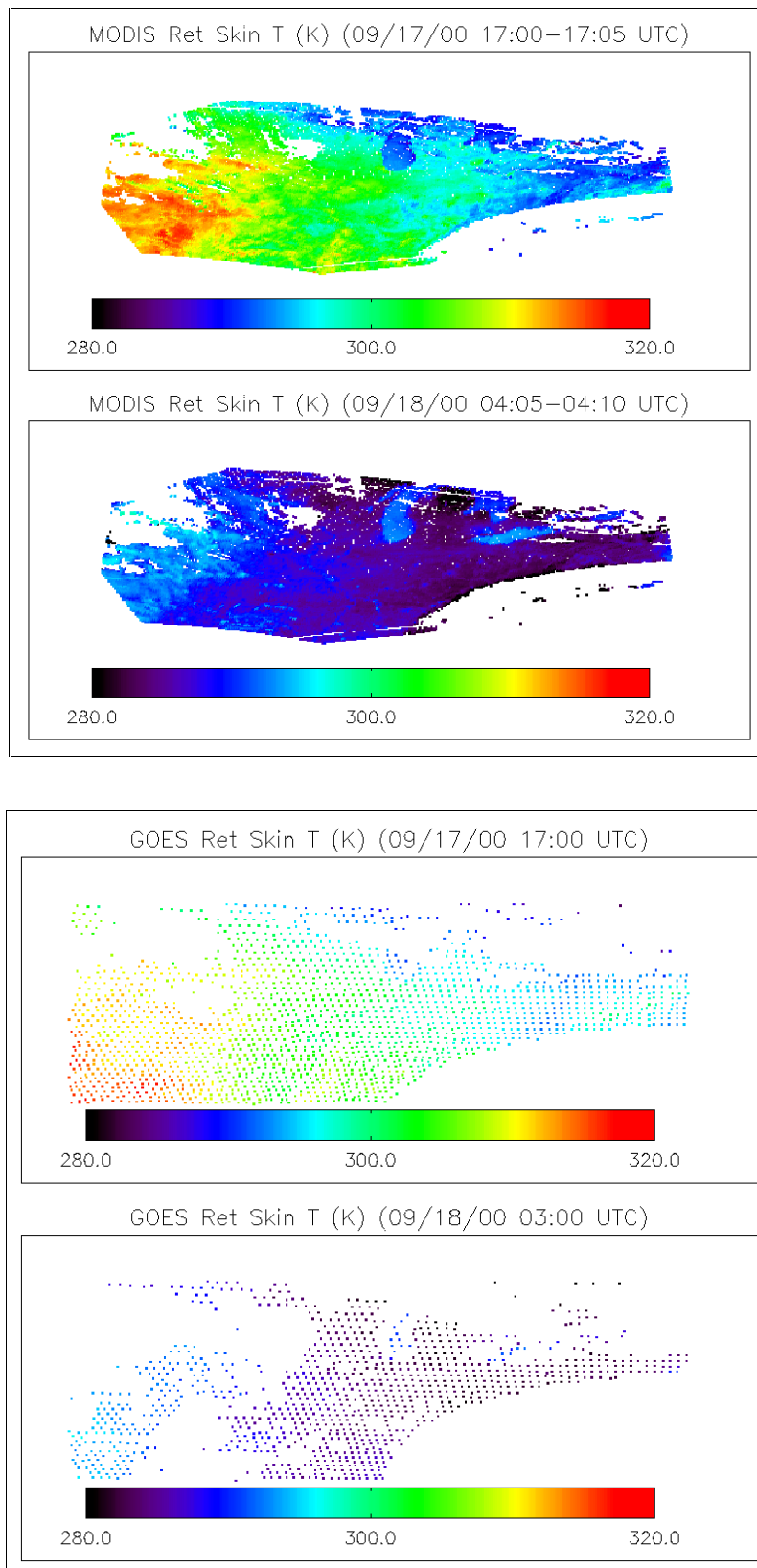
Figure 17: Retrieved surface skin temperature from MODIS (top) and GOES (bottom) respectively in the overlap region for 17 day and 18 night September 2000.
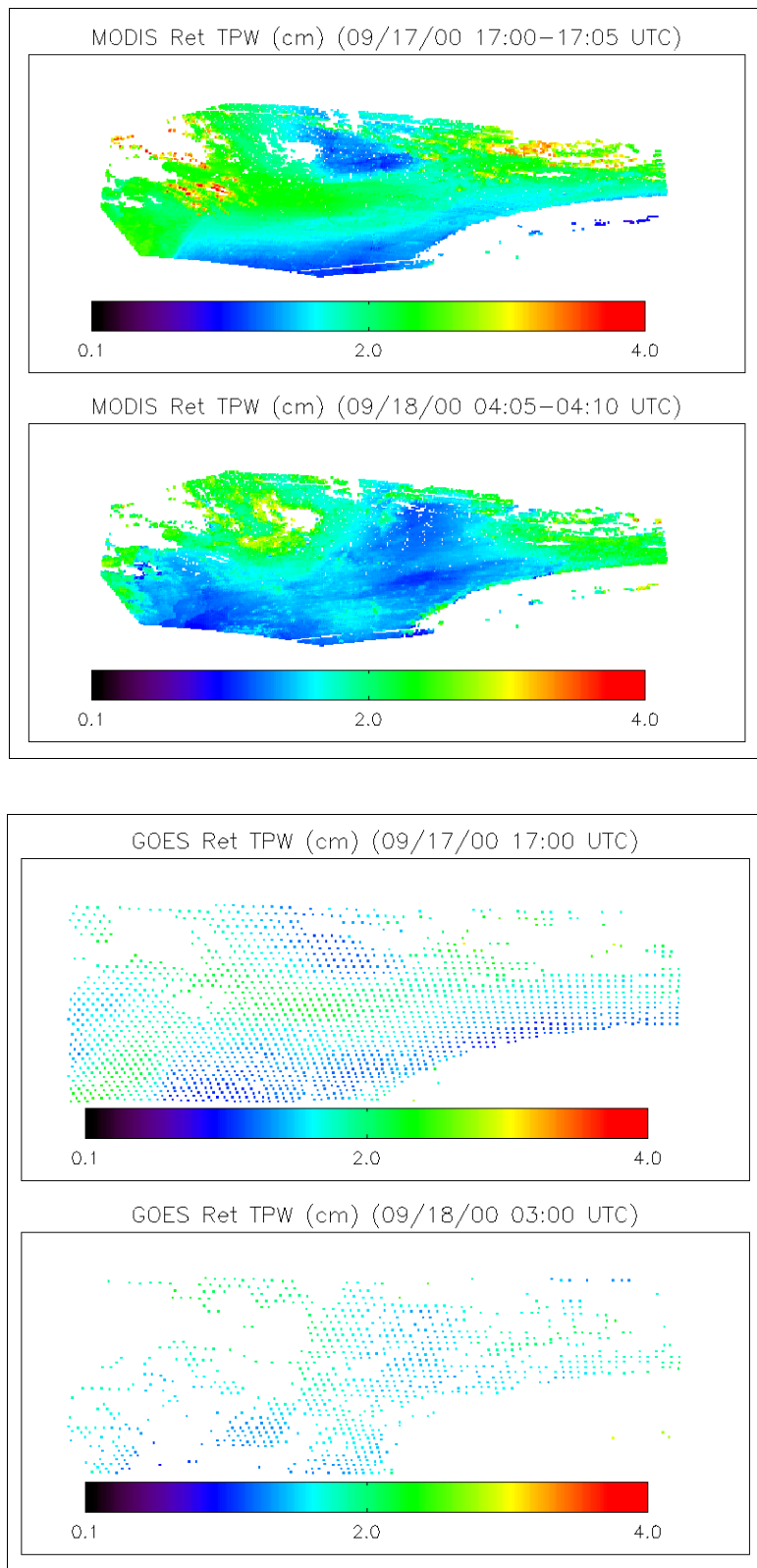
Figure 18: Retrieved total precipitable water vapor from MODIS (top) and GOES (bottom) in the overlap region for 17 day and 18 night September 2000.
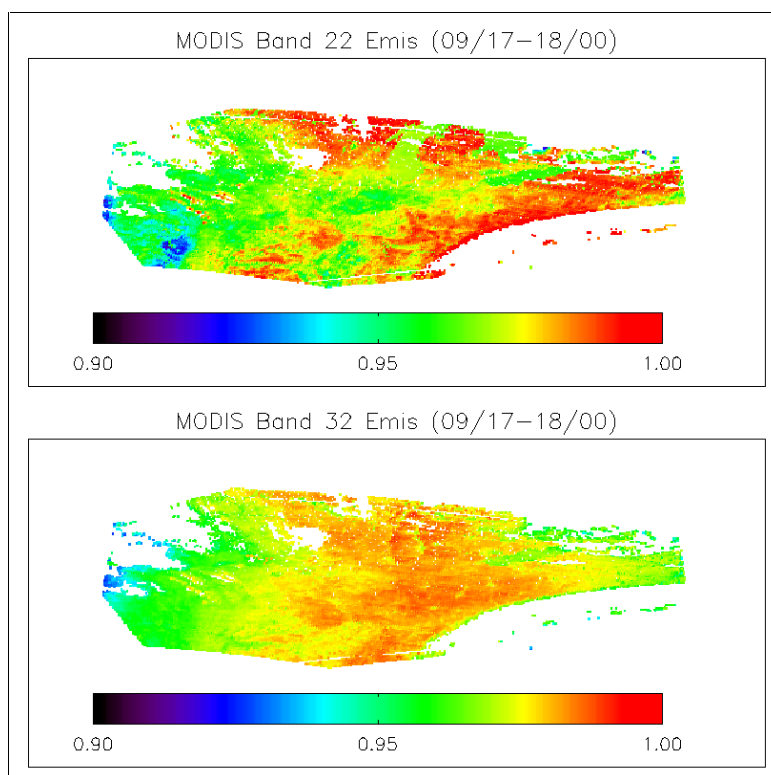
Figure 19: Retrieved surface shortwave (top) and longwave (bottom) emissivity from MODIS for 17 - 18 September 2000.

MEETINGS

Liam Gumley presented an interactive poster entitled "EOS Direct Broadcast Reception and Processing at the University of Wisconsin-Madison" at IGARSS 2000, Honolulu, Hawaii, July 24-28.

P. Menzel presented a paper on "Early MODIS Atmospheric Science Products: Radiances, Cloud Detection, Cloud Properties, and Atmospheric Profiles" at the International Radiation Symposium held 24 – 29 July 2000 in St. Petersburg, Russia.

Dan LaPorte attended the 2000 Conference on Characterization and Radiometric Calibration for Remote Sensing held in Logan, UT, September 2000.

Liam Gumley gave a keynote address entitled "Atmospheric Applications of Terra MODIS at the University of Wisconsin-Madison" at the 10th TeraScan Users Conference, La Jolla, California, October 17-19.

Liam Gumley attended the NPOESS Preparatory Project (NPP) Data System Workshop at NASA GSFC, Greenbelt, Maryland, November 30 – December 1.

PAPERS

Ma, Xia Lin, Z. Wan, C. C. Moeller, W. P. Menzel, L. E. Gumley, and Y. Zhang, Retrieval of geophysical parameters from Moderate Resolution Imaging Spectroradiometer thermal infrared data: evaluation of a two-step physical algorithm. Applied Optics, V39, No. 20, pp. 3537-3550, 2000.

Menzel, W. P. and Y. Plokhenko, 2000: Accounting for the effects of surface emissivity in profile retrievals from infrared multispectral radiances. Presented at the International Radiation Symposium held 24 – 29 July 2000 in St. Petersburg, Russia.

Moeller, C. C., D. D. LaPorte, W. P. Menzel, H. E. Revercomb, R. O. Knuteson, and M. D. King: Comparison of early Terra MODIS emissive band radiances with collocated ER-2 based SHIS and MAS measurements. Presented at the IEEE 2000 IGRSS Symposium, Honolulu, HI, July 2000.

Nasiri, S. L., B. A. Baum, A. J. Heymsfield, P. Yang, M. R. Poellot, D. P. Kratz, and Y. Hu, 2000: The Development of Midlatitude Cirrus Models for MODIS Using FIRE-I, FIRE-II, and ARM In-Situ Data. Submitted to the Journal of Applied Meteorology.

X. Xiong, T. Dorman, S. Xiong, K. Chiang, Y. Zhang, B. Guenther, C. Moeller: Using the moon for the on-orbit determination of MODIS PC bands optical leak. Presentation to the 2000 Conference on Characterization and Radiometric Calibration for Remote Sensing, SDL/USU, Logan, UT, September 19 - 21, 2000

Yang, P., B.-C. Gao, B. A. Baum, W. Wiscombe, Y. Hu, S. L. Nasiri, A. Heymsfield, G. McFarquhar, and L. Miloshevich, 2000: Sensitivity of cirrus bidirectional reflectance in MODIS bands to vertical inhomogeneity of ice crystal habits and size distributions. In press, J. Geophys. Res.

Yang, P., B.-C. Gao, B. A. Baum, W. Wiscombe, M. I. Mischenko, D. M. Winker, and S. L. Nasiri, 2000: Asymptotic solutions of optical properties of large particles with strong absorption. In press, Applied Optics.

Yang, P., B.-C. Gao, B. A. Baum, Y. X. Hu, W. J. Wiscombe, S.-C. Tsay, and D. M. Winker: Radiative properties of cirrus clouds in the infrared (8-13 microns). In press, J. Quant. Soc. Rad. Trans.